Nanoscale

RSC Publishing

PAPER

View Article Online
View Journal | View Issue

Analysis of copper nanoparticles toxicity based on a stress-responsive bacterial biosensor array†

Cite this: *Nanoscale*, 2013, **5**, 653

Fenfang Li, Chunyang Lei, Qinpeng Shen, Lijun Li, Ming Wang, Manli Guo, Yan Huang,* Zhou Nie* and Shouzhuo Yao

The rapid development in nanoparticle production and application during the past decade requires an easy, rapid, and predictive screening method for nanoparticles toxicity assay. In this study, the toxicological effects and the source of toxicity of copper nanoparticles (CuNPs) are investigated based on a stress-responsive bacterial biosensor array. According to the responses of the biosensing strains, it is found that CuNPs induce not only oxidative stress in *E. coli*, but also protein damage, DNA damage, and cell membrane damage, and ultimately cause cell growth inhibition. Through enzyme detoxification analysis, the toxicological effects of CuNPs are traced to H_2O_2 generation from CuNPs. Rapid copper release from CuNPs and Cu(I) production are observed. The oxidation of the released Cu(I) has a close relation to H_2O_2 production, as tris-(hydroxypropyltriazolylmethyl) amine, the specific Cu(I) chelator, can largely protect the cells from the toxicity of CuNPs. In addition, the TEM study shows that CuNPs can be adsorbed and incepted fast by the cells. Comparatively, copper microparticles are relatively stable in the system and practically non-toxic, which indicates the importance of toxic estimation of materials at the nanoscale. In addition, the Cu(II) ion can induce protein damage, membrane damage, and slight DNA damage only at a relatively high concentration. The current study reveals the preliminary mechanism of toxicity of CuNPs, and suggests that the stress-responsive bacterial biosensor array can be used as a simple and promising tool for rapid screening *in vitro* toxicity of nanoparticles and studying the primary mechanism of the toxicity.

Received 5th August 2012
Accepted 8th November 2012

DOI: 10.1039/c2nr32156d

www.rsc.org/nanoscale

1 Introduction

Safety evaluation of engineered nanomaterials is important to the sustainable development of the nanotechnology industry. Compared to the rapid development of the synthesis technology and broad application, the risk estimation of using nanomaterials for human health and the environment has not yet been fully established, although it has attracted considerable concern. Nowadays, the traditional toxicological approaches, which involve animal experiments and cellular viability assays, are still the major means to estimate the toxicity of nanomaterials.[1–4] Animal studies can assess the safety of chemicals and further extend that to human being. Nevertheless it is expensive, time-consuming, and labor-intensive, making it hard to meet the analytical demands when confronted with thousands of new nanomaterials. As to the widely used *in vitro* methods, such as MTT, LDH and Neutral red assays, these cellular viability assays are based on determining different aspects of cellular toxicity, making it difficult to compare the data.[5] Moreover, in view of the extraordinary properties of nanomaterials, such as reacting with or adsorbing the assay components by themselves, these *in vitro* methods are less suitable to addressing nanomaterial-derived cytotoxic effects.[5] Currently, systemic biological approaches, including genomics, proteomics, and metabonomics/metabolomics, have been applied in the toxicology research field.[6] However, the expensive instrumentation limits the wide spread of these approaches.

Stress-responsive bacteria are recombinant ones, which respond to several classes of threats (stresses) with signal production (Fig. S1†).[7–10] In these bacteria, the reporter genes are fused to and under the control of different stress-responsive promoters of the bacteria (a promoter is a region of DNA that regulates the transcription of a particular gene downstream). When these biosensor strains are exposed to compounds or conditions that are toxic to induce stresses in the bacteria, the related global regulatory systems containing the stress-inducible activator protein genes and the stress-responsive promoters will be activated, for instance, the SOS system responds to DNA damage, and the heat shock system responds to protein damage. Therefore the "tailored" bacteria can recognize the stress with the stress-responsive promoters and turn on the transcription of the reporter gene, and then the corresponding protein product, fluorescent protein or luciferase, can produce

State Key Laboratory of Chemo/Biosensing and Chemometrics, College of Chemistry and Chemical Engineering, Hunan University, Changsha, 410082, P. R. China. E-mail: huangyan.hnu@gmail.com; niezhou.hnu@gmail.com

† Electronic supplementary information (ESI) available. See DOI: 10.1039/c2nr32156d

easily detectable signals like fluorescence and luminescence.[8,11] Simple growth and maintenance, and rapid response of the engineered bacteria make themselves low-cost, easy and rapid to detect toxins. In addition, the strains can provide information on the toxic character of the analytes at the transcriptional level and their bioavailability.[7,10] With such bacteria, the toxicity of some environmental pollutants (*e.g.* heavy metals, endocrine disrupting chemicals) has been successfully evaluated.[12,13] Recently, the toxic mode of silver nanoparticles was also analyzed according to the cellular responses of the whole-cell sensing bacteria.[14] Accordingly, the stress-responsive bacteria have the potential to form a biosensor array to investigate nanoparticles toxicity.

Copper nanoparticles (CuNPs) are one of the most important engineered nanoparticles (NPs). Because of their excellent optical, electrical, catalytic, and antimicrobial properties, they are widely used in electronics, ceramics, films, polymers, inks, metallics, and coatings.[15–17] CuNPs also have wide applications in osteoporosis-treatment drugs and additives of livestock and poultry feed.[6] With the increased production and wide application of CuNPs, which leads to a wide spread of them in the environment, their effect on the ecosystem as well as on human health has attracted much attention. Previous animal studies have demonstrated that CuNPs produce hepatotoxicity, nephrotoxicity and heavy injury in the spleens of experimental mice and rats,[3,6] and induce gill toxicity in zebrafish.[4] The results from such *in vitro* analysis as comet assays and Trypan blue staining suggested that CuNPs cause DNA damage and cytotoxicity.[18] Although the toxic effects of CuNPs were reported[3,4,6,19,20] the toxic mechanism of CuNPs, which is important for assessment of their impact on human health and the environment, still needs further investigation.

In the present work, a panel of stress-responsive *E. coli* was used as a combination in a microtiter plate to form a stress-responsive bacterial biosensor array. With this biosensor array, the toxicological effects and source of the toxicity of CuNPs were analyzed, and compared with that of copper microparticles (CuMPs) and dissoluble copper ion ($CuCl_2$). This biosensor array includes a panel of genetic engineered *E.coli*, where stress-specific promoters, such as P_{katG}, P_{recA}, P_{fabA}, and P_{grpE}, were fused to the *luxCDABE* operon. The reporter protein, bacterial luciferase, which is encoded by the *luxCDABE* operon from *Vibrio fischeri*, has several advantages, such as high sensitivity, no substrate needed, and no endogenous activity in the host cell, *E.coli*.[21] These sensing strains are *E.coli* DPD2511 (*katG::luxCDABE*), responsive to oxidative damage, DPD2794 (*recA::luxCDABE*), responsive to DNA damage, DPD2540 (*fabA::luxCDABE*), sensitive to perturbations of fatty acid synthesis, and TV1061 (*grpE::luxCDABE*), sensitive to protein damage. With optimization of this system, the toxicological effects of CuNPs were assayed in about half an hour after exposure. With the help of the reactive oxygen species (ROS) scavenge enzymes and the specific Cu(I) chelator, this system was used to elucidate the primary mechanism of the toxicity of CuNPs. As far as we know, the present study is the first holistic investigation on the toxicological effects of CuNPs as well as the primary mechanism of toxicity of CuNPs.

2 Experimental details

2.1 Materials

CuNPs used in this study were purchased from SuZhou-CanhuoNano Technology Co. Ltd, China. CuMPs, $CuCl_2 \cdot 6H_2O$ and hydrogen peroxide were obtained from Sinopharm Chemical Reagent Inc., China. 2,9-Dimethyl-1,10-phenanthroline (the neocuproine reagent), superoxide dismutase (SOD) and catalase (CAT) were bought from Sigma, USA. All the chemicals used were analytical grade.

2.2 Particles preparation and dispersion

Hermetically stored CuNPs were divided into several parts and stored under air-free conditions, where particles were protected by dry argon gas until the experiments. CuNPs solutions were freshly prepared before use. For good dispersion, the solutions containing CuNPs were sonicated for 2×10 s with a 3 s pause using a JY92-IIN ultrasonic cell disruption system (Scientz, China), and then diluted further to specified concentrations during exposure. CuMPs were directly added into the test solution in specified concentrations.

2.3 Particles characterizations

The specific surface area of particles was determined by means of BET analysis with a Monosorb (Quantachrome,USA) instrument. The powder XRD patterns of the samples were recorded by a X-ray diffractometer (*D*/max 2550VB+18KW, Rigaku, Japan) using Cu Kα (40 kV, 250 mA) radiation ($\lambda = 1.54178$ Å) at a scanning rate of 2.4° min^{-1} for 2θ ranging from 10–85°. The microstructures and morphologies were investigated by a scanning electron microscope (SEM, JSM-6360, JEOL, Japan) with energy dispersive X-ray (EDX) detector working at 25 kV. X-ray photoelectron spectroscopy (XPS) was carried out on an X-ray photoelectron spectrometer (K-Alpha 1063, Thermo Fisher, USA) using Al Kα X-rays as the excitation source. Size distribution and zeta potential of particles in the cell medium were analyzed with a Nano Zetasizer (Malvern, UK).

2.4 Bacterial strains and culture conditions

The *E. coli* strains used in this work were kindly donated by Prof. Belkin and are shown in Table 1. These recombinant bioluminescence strains were grown aerobically on a rotary shaker (200 rpm) at 30 °C in Luria-Bertani (LB) broths or on LB plates containing 25 μg ml^{-1} kanamycin sulfates. The host strain

Table 1 Description of the bacterial strains used in this study

Strains	Plasmid	Host	Response	Ref.
RFM443	N/A[a]	RFM443[b]	N/A	8
DPD2511	P_{katG} Lux	RFM443	Oxidative damage	8
DPD2794	P_{recA} Lux	RFM443	DNA damage	7
DPD2540	P_{fabA} Lux	RFM443	Membrane damage	9
TV1061	P_{grpE} Lux	RFM443	Protein damage	10

[a] No recombinant plasmid. [b] Genotype of RFM443 is (StrR, *galK*2 *lac*_74 *rpsL200*).

RFM443 was cultured at 37 °C in LB medium without kanamycin sulfates.

2.5 Toxicity assays

The toxicities of CuNPs and Cu(II) were assayed in both microtiter plate and flask, while the toxicity assays of the CuMPs were performed only by flask tests, since the big particles cannot be dispersed well in liquids and also cannot be diluted in solutions. For the microtiter-plate assay, the overnight cultures of all kinds of strains as seeds were firstly diluted 100-fold with fresh LB in the test tube, and grown in a rotary shaker at 30 °C for the optimized time. Secondly, 98 μL portions of the bacterial cultures were transferred to wells of an opaque black 96-well microtiter plate, and then mixed with 2 μL of different dilution series of analytes/inducers, which were dissolved in LB medium. LBs containing different dilution series of CuNPs only were rotary shaken at 30 °C for 0.5 h and the supernatants were collected by centrifugation and worked as one kind of inducers. Finally, the microtiter plate was placed in a Synergy™ Mx SMATLD Multi-Mode Microplate Reader (Biotech, USA) and continuously shaken at 30 °C. Absorbance at 600 nm and bioluminescence were measured at 5 min intervals during the experiment. For the flask assay, the strains were cultured in the same way as aforementioned, except a flask was used. After that, these cultures were mixed directly with analytes/inducers of various concentrations and incubated at 30 °C. After each 5 min 100 μL mixtures were transferred into 96-well-microtiter plates with a transparent bottom, and absorbance at 600 nm and bioluminescence were read by Synergy™ Mx SMATLD Multi-Mode Microplate Reader. Similar assays under the same conditions but without the analytes/inducers were performed as negative controls. The RLUmax (the maximum of Relative Luminescence Unit) in this study is defined as the ratio of the maximum luminescence from the induced cells to that from control cells.

2.6 Bacterial sample preparation for transmission electron microscope

The cell culture exposed to CuNPs for 0.5 h was collected by centrifugation and fixed in 2.5% glutaraldehyde for 4 h. Then the mixture was centrifuged and rinsed with PBS (0.1 M, pH 7.2) 5 times. The pellet was re-suspended in PBS containing 1% osmium tetroxide and kept at 4 °C for 2 h, and was gradually dehydrated by ethanol for 20 min 3 times. The resulting dehydrated sample was embedded in epoxy resin (Kit Embed 812, Euromedex, France) and dried for 12 h at 40 °C, and another 12 h at 60 °C. After that, the sample was cut on an Ultracute (AO-E, USA) to get thin sections. The TEM grid was a 150-mesh carbon-coated nickel TEM grid. TEM (JEM-2100F, JEOL, Japan), accompanied with EDX, was used to analyze the bacterial thin sections and the relative position of the bacteria and CuNPs.

2.7 Enzyme detoxification analysis

The procedure of enzyme detoxification analysis was similar to the toxicity assay of CuNPs except that the enzyme(s), catalase (CAT) or/and superoxide dismutase (SOD), was/were added with CuNPs into the cell cultures. Final concentrations of catalase and superoxide dismutase were both 200 U mL^{-1}.

2.8 Copper release analysis

The copper release properties of CuNPs and CuMPs in LB medium were analysed using an atomic absorption spectrophotometer (7JO-8024, Hitachi Z-2000, Japan). The particles immersed in the medium were shaken under conditions similar to that of the toxicity assays. For release kinetics of the particles, 20 mg L^{-1}, 80 mg L^{-1} and 200 mg L^{-1} of CuNPs and 200 mg L^{-1} of CuMPs, respectively, were incubated with cells or without cells in the LB medium. After exposure for some specific time, particles were separated from the media by centrifugation for 10 min at 22 000*g*, and then the supernatants were collected and filtered through a 0.22 μm cellulose filter (Millipore, USA). Resulting samples were investigated for their soluble copper by AAS.

2.9 Cuprous ion detection

To check the production of Cu(I) from CuNPs, neocuproine agent (Nc), a selective Cu(I) chelator, was used. 20 mg L^{-1} of CuNPs, CuMPs, $CuCl_2 \cdot 6H_2O$ or the supernatant of CuNPs-containing LB medium, respectively, was added into LB medium containing 60 mg L^{-1} Nc. Then the complexes were mixed and kept at room temperature for 5 min. After centrifuging for 10 min at 22 000*g*, the obtained supernatants were investigated for absorbance against a reagent blank by UV–Vis spectrophotometer (DU-800, Beckman, USA).

2.10 THPTA detoxification analysis

THPTA was synthesized according to the procedure of Liu *et al.*[46] The THPTA detoxification assay was similar to the enzyme detoxification analysis. This water-soluble cuprous chelator, instead of CAT or SOD, together with CuNPs was added into the cell cultures to illustrate the role of Cu(I) in the toxicity of CuNPs. Excess THPTA (12.5 mM), compared to the concentration of CuNPs, was used.

3 Results and discussions

3.1 Optimization of the biosensor array

On account of their abilities to respond to different kinds of stresses and produce luminescence signals, four recombinant strains, listed in Table 1, were selected to compose the bacterial biosensor array. It was reported that these strains are more sensitive to different kinds of stresses than other microbial toxicity tests like Microtox™,[22] whereas the maximum response time of these strains was relatively longer and varied with the strain. Since the metabolic activity of bacteria is closely related to their growth phase, the strains were pre-cultured for different times, and then were exposed to different kinds of representative stress-induce compounds, including hydrogen peroxide (H_2O_2) (oxidative stress), mitomycin (DNA damage), phenol (membrane damage), and ethanol (protein damage). The luminescence signals were recorded by a Synergy™ Mx SMATLD Multi-Mode Microplate Reader (Biotech, USA). RLU_{max}, defined

as the ratio of the maximum luminescence emitted from the induced strain to that from a non-induced strain, was calculated to value the response of the tested strain to a tested compound. According to the growth curve of the strains, 1, 1.5, 2, 2.5 and 3 h, which are in the early exponential phase of the strains, were selected as pre-culture time. As shown in Fig. S2,† pre-culture time does influence responses of the strains in the presence or absence of different representative stress-induce compounds. 1.5 h, 1 h, 1 h, and 1.5 h were chosen as the optimized pre-culture time for DPD2511, DPD2794, DPD2540 and TV1061, respectively, to get maximum RLUmax (Fig. 1). With these optimized pre-culture times, not only are the sensitivities of the strains dramatically improved, which are about 14–30 times higher compared with a 3 h pre-culture time, but also all the strains respond to CuNPs immediately after exposure, and the maximum response time of the strains to CuNPs was approximately 0.5 h (Fig. S3†). Such modified manipulation of the biosensing bacteria combined with a microtiter plate luminometer presents a sensitive and easy screening method to study toxicological effects of CuNPs in a short time.

3.2 Toxicity of CuNPs

Since cytotoxic effects reflect the holistic damage induced by the particles, we tested the cytotoxicity of CuNPs as well as CuMPs and soluble Cu(II) ($CuCl_2$was added) with the host strain *E. coli* RFM443. The spherical CuNPs (12.45 $m^2\ g^{-1}$, Fig. 2A and 2a) and CuMPs (0.21 $m^2\ g^{-1}$, Fig. 2B) have a primary particle size of about 90 nm and 10 μm, respectively, and are homogeneous and highly crystalline (Fig. 2C and 2D), while exposure to the ambient atmospheric conditions makes both surfaces be partly oxidized to CuO (Fig. S4†). After 3 h exposure to CuNPs at various concentrations of 20, 40, 60, 80, 100, 120, 140, 160, 180 and 200 mg L^{-1}, the growth of RFM443 was obviously inhibited. For instance, the growth rate of RFM443 with the lowest loading of 20 mg L^{-1} CuNPs was only 93% that of the control experiment without CuNPs, and the higher the concentration of CuNPs, the slower the growth of the strain (Fig. 3 and S5†). It is also shown that CuNPs induce heavier injury in RFM443 than Cu(II) and CuMPs at equal mass concentrations. 58% and 50% growth inhibition of RFM443 were observed for 200 mg L^{-1} CuNPs and Cu(II), respectively, while CuMPs at the same concentration did not notably affect the growth rate of the strain.

To investigate the toxicological effects of CuNPs at a transcriptional level, the panel of whole-cell bacterial biosensing strains was exposed to CuNPs at the same concentrations in the cytotoxicity assay. Fig. 4 presents that all of the strains, DPD2511, DPD2794, DPD2540, and TV1061, emitted luminescence when they were mixed with CuNPs in the experimental concentration range, indicating that CuNPs could cause

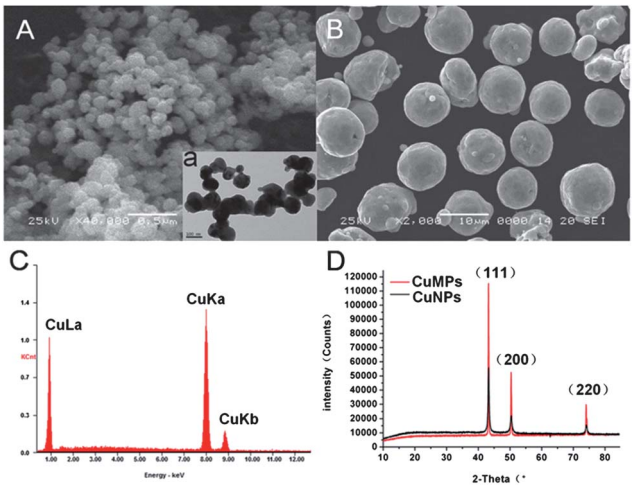

Fig. 2 Scanning electron microscope (SEM) (A) and energy dispersive X-ray (EDX) (C) analysis of CuNPs, the SEM image of CuMPs (B), and their corresponding X-ray diffractometer (XRD) spectra (D). Inset is the transmission electron microscope (TEM) image of CuNPs (a).

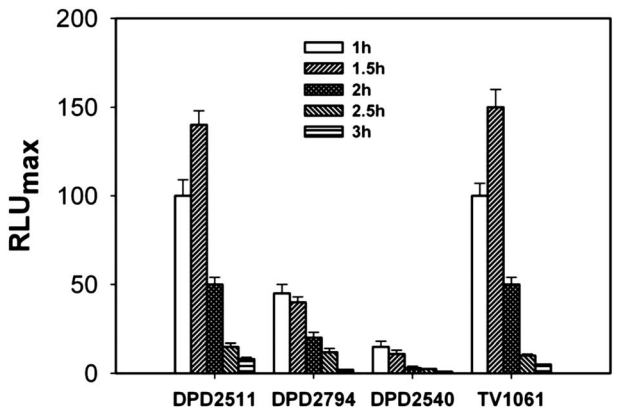

Fig. 1 Comparison of responses of four biosensing strains with different pre-culture times. The strains were exposed to their representative stress-induce compounds. DPD2511 was exposed to 30 mg L^{-1} hydrogen peroxide, DPD2794 to 2 mg L^{-1} mitomycin, DPD2540 to 100 mg L^{-1} phenol, and TV1061 to 3% ethanol. Each data point is an average of three individual replicates, with error bars denoting the standard deviation.

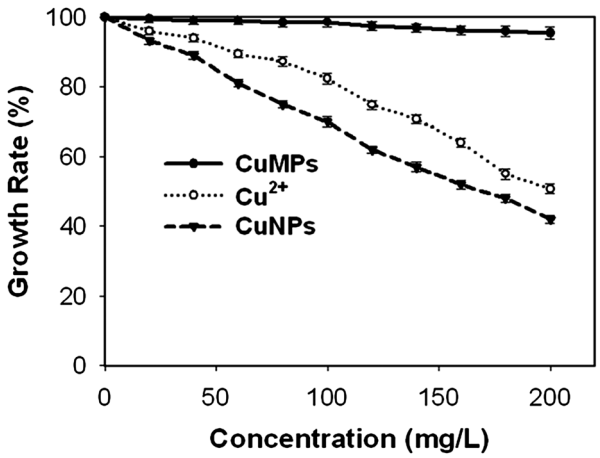

Fig. 3 Specific growth rate of the host strain *E. coli* RFM443 in the presence of different concentrations of CuNPs, CuMPs and Cu(II). The *y* axis is the ratio of growth rate of *E. coli* RFM443 in LB medium with the inducers to that of it without the inducers. Each data point is an average of three individual replicates, with error bars denoting the standard deviation.

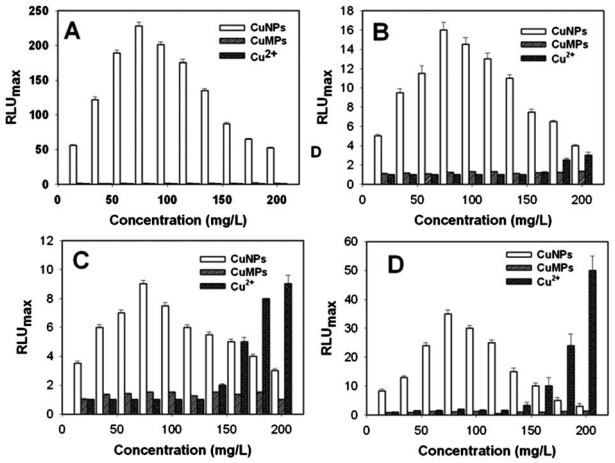

Fig. 4 Responses of (A) DPD2511, (B) DPD2794, (C) DPD2540 and (D) TV1061 to different concentrations of CuNPs, CuMPs and Cu(II). Each data point is an average of three individual replicates, with error bars denoting the standard deviation.

oxidative stress, DNA damage, membrane damage, and protein damage in the tested strains, and the related promoters responded to these damages, and then turned on the transcription of the reporter gene. Moreover, CuNPs induced luminescence of all the tested strains in a similar dose-dependent manner with the maximal effect at the same concentration of CuNPs (80 mg L^{-1}) (Fig. 4 and S3†). This peak-shaped profile of strain response *versus* CuNPs concentration is probably attributed to the balance of two opposing influences: (1) the increasing signal protein generation in response to the increase of CuNP-induced damage and (2) the heavier inhibition of cellular metabolism and growth caused by more CuNPs. When concentration of CuNPs is low, the response from strains increases with the concentration of CuNPs, since the metabolism and growth of cells are not deeply affected by this range of concentrations of CuNPs. With high concentrations of CuNPs, the viability of cells is significantly lost or signal synthesis related metabolism is heavily inhibited, and hence, a reduction of transcriptional level and a decrease of luminescence. Compared with CuNPs, CuMPs showed totally different effects on cells and no obvious responses of any strains were observed (Fig. 4), although these two kinds of particles have the same chemical composition. This result indicates that the CuMPs are almost harmless, which is in accordance with the above cytotoxicity result that there is nearly no effect of CuMPs on cell growth (Fig. 3). The response of the strains to Cu(II) ion is different to CuNPs and CuMPs. DPD2511 showed no signal response in the entire experimental concentration range of Cu(II) and the other three strains emitted little luminescence in 0–140 mg L^{-1} Cu(II) (Fig. 4). The significant signal increase of TV1061 and DPD2540 was started at 140 mg L^{-1} Cu(II), and the signal became higher than that of CuNPs at above 160 mg L^{-1} Cu(II) (the signals of TV1061 and DPD2540 to 200 mg L^{-1} Cu(II) were 16 and 2 fold higher than that to 200 mg L^{-1} CuNPs, respectively). In the DPD2794 strain, the similar dose-dependent signal increase was also observed when the Cu(II) concentration was higher than 160 mg L^{-1}, but the signals were lower than for CuNPs. These results imply that the major toxic effects of Cu(II) ion are membrane damage and protein damage, which occur only at high concentrations (>140 mg L^{-1}), whereas CuNPs cause all four kinds of damaging effects at low concentrations (maximum at 80 mg L^{-1}). Therefore, CuNPs possess higher bio-toxicity to the ecosystem than CuMPs and Cu(II) due to their multifaceted and intensive damage effects with much lower toxic concentrations. Moreover, the different concentration profile and damage effects between CuNPs and Cu(II) ion suggest that the toxic mechanism of CuNPs probably does not depend on Cu(II) ions.

3.3 H_2O_2 is a major toxic source for CuNPs

Currently, reactive oxygen species (ROS) generation is considered as the best developed paradigm for nanoparticle toxicity,[23–26] in the respect that these kinds of particles have special electronic configurations or surface properties to allow spontaneous ROS generation, contain oxidizable components that can release electrons to form ROS, or can interact with cellular components to generate oxidative stress.[23] H_2O_2 is one kind of ROS, which can induce the transcription of the *oxyR* regulon in *E. coli*, and *katG* belongs to this H_2O_2-sensitive *oxyR* regulon.[8] The above result that the oxidative stress-sensitive strain DPD2511 (*katG::luxCDABE*) was intensively induced by CuNPs (Fig. 4A) indicates that H_2O_2 was produced from CuNPs. To further confirm the H_2O_2 generation, enzyme detoxification analysis was carried out with catalase (CAT), an enzyme that converts H_2O_2 into oxygen and water molecules. As shown in Fig. 5, the luminescence of DPD2511 induced by CuNPs is completely abolished by the addition of CAT. The other three strains (DPD2540, DPD2794, TV1061) also show significantly reduced responses (about 78–90%) as CAT eliminated H_2O_2. Furthermore, growth of strain RFM443 inhibited by CuNPs was largely resumed by the addition of CAT (Fig. S6†), which affirms that H_2O_2 is a major toxicological source for CuNPs. Since H_2O_2 is one kind of relatively inert ROS, toxicity of CuNPs was compared with that of H_2O_2 directly. 30 mg L^{-1} H_2O_2 was

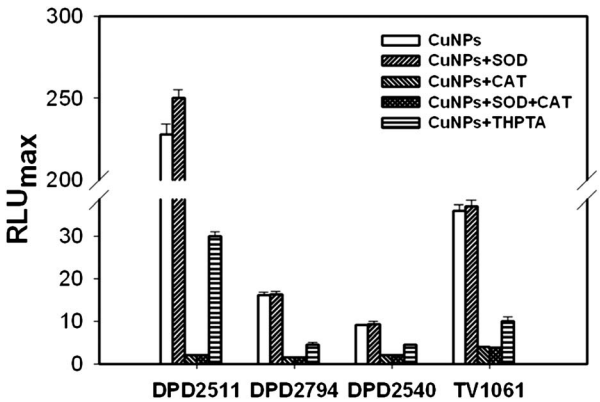

Fig. 5 Detoxification assays of CAT, SOD, and THPTA. The stress-respective biosensing bacteria (DPD2511, DPD2794, DPD2540 and TV1061) were exposed to CuNPs alone, or together with SOD and/or CAT, and THPTA, and the responses of these strains were recorded. Each data point is an average of three individual replicates, with error bars denoting the standard deviation.

chosen because it can induce an equivalent response of DPD2511 to 80 mg L^{-1} CuNPs (Fig. S7A†). As expected, all the recombinant strains responded to H_2O_2 (Fig. S7B†). The luminescence from DPD2540 and TV1061 induced by H_2O_2 were a little weaker than that by CuNPs, which is consistent with that only about 20% of the signal remains after CAT treatment observed in the detoxification analysis (Fig. 5). The genotoxicity sensitive strain, DPD2794, responded more strongly to H_2O_2 than to CuNPs (Fig. 5), possibly because the Cu(II) released from CuNPs can decrease DNA damage rate of H_2O_2 through elimination of iron-mediated oxidation.[27] Thus the results of H_2O_2 elimination experiments demonstrate that H_2O_2 generation caused by CuNPs probably acted as the major source of CuNPs toxicity, causing not only oxidative stress in the bacteria, but also DNA damage, membrane damage, and protein damage. This is also a probable reason that the biosensing strains showed similar dose-dependent responses to CuNPs (Fig. 4).

Furthermore, to examine if another major ROS, superoxide ion radical (O^{2-}), is produced by CuNPs, superoxide dismutase (SOD) was added into the analytical systems. The presence of SOD caused a 10% signal increase of DPD2511 and slight increasing response of other strains to CuNPs (Fig. 5), while it did not change the growth inhibition of RFM443 caused by CuNPs (Fig. S6†). The two enzymes, SOD and CAT, worked together reducing a little more responses of strains DPD2540, DPD2794, and TV1061 than CAT alone did (Fig. 5). Since SOD catalyzes the reaction that transforms O^{2-} into H_2O_2, the above data suggest that a small quantity of O^{2-} was generated from CuNPs in the culture, and induced rather limited oxidative stress, DNA damage, protein damage and membrane damage, but not cytotoxicity, and these results further confirm that the toxicity of H_2O_2 plays a key role in the system.

3.4 Correlation of CuNPs toxicity with release properties

Metal fraction release largely contributes to the toxicity of metal nanoparticles in a water environment.[28] Several studies reported that the observed toxic effects induced by ZnO nanoparticles were mainly explained by dissolved Zn ions.[29,30] Torsi *et al.* demonstrated that bioactivity of copper nanoparticle–polymer composites correlated with the released copper into the culture broth.[31] Thus analysis of copper release from CuNPs in conditions similar to the toxicity test was performed to estimate the relationship between copper release and CuNPs toxicity.

First of all, the release kinetics of CuNPs was investigated by atomic absorption spectrophotometry (AAS). As depicted in Fig. S8†, CuNPs exhibit a high release rate in the first 1 h, and the dissolution increases with the increased initial particle concentration, while the release rate decreases in parallel. For example, 75% and 72% copper was released in the culture medium containing 20 and 80 mg L^{-1} CuNPs (corresponding to 15 and 58 mg L^{-1} soluble Cu, respectively) in 1 h, and a slower copper release of 50% was observed at 200 mg L^{-1} CuNPs (corresponding to 100 mg L^{-1} soluble Cu). After that, the copper release gradually reached equilibrium. Such a high degree of copper dissolution was also found when CuNPs were exposed in DEME+ medium.[18] According to the previous report that the amino acid-rich components, such as yeast extract and tryptone, mediated copper leaching from CuO NPs, but not CuO MPs,[32] we suppose that such components also affect the copper release from CuNPs, as both DEME+ and LB are amino acid-rich media. The release rate of CuMPs was much lower than that of CuNPs, and only 1.3% copper was released from 200 mg L^{-1} CuMPs (corresponding to 2.6 mg L^{-1} soluble Cu, Fig. S8†) in 1 h. The presence of *E. coli* did not change the release kinetic of CuNPs a lot, and the small decrease of copper dissolution was possibly due to nutrient consumption or copper uptake by the bacteria. Furthermore, at the first 30 min, when the maximum response of the sensing bacteria to CuNPs approximately happened, 14, 40, 70 and 1.3 mg L^{-1} soluble Cu was detected at 20, 80, and 200 mg L^{-1} CuNPs, and 200 mg L^{-1} CuMPs, respectively. By comparison with the data in Fig. 4, these soluble coppers, if they are Cu(II), cannot induce any detectable response of the recombinant luminescent bacteria.

Secondly, since both cupric and cuprous ions were detected by AAS, production of Cu(I) from CuNPs was further checked. 2,9-dimethyl-1,10-phenanthroline (neocuproine, Nc), a selective Cu(I) chelator, was chosen to check the existence of Cu(I) *in vitro*. According to UV–visible spectral analysis (Fig. 6), a new complex with the maximum absorption at 457 nm, the specific absorption of Nc–Cu(I) complex,[33] was produced when Nc (60 mg L^{-1}) and CuNPs (20 mg L^{-1}) co-existed in the medium, confirming the production of Cu(I) from CuNPs. Similar to copper release, a slightly decreased Cu(I) leaching from CuNPs was observed when the *E. coli* cells existed in the medium (Fig. 6). There was no specific complex created after CuMPs or Cu(II) was immersed in the medium with neocuproine (Fig. 6), implying there was no Cu(I) generated.

Thirdly, contribution of Cu(I) to the toxicity of CuNPs was analyzed with tris-(hydroxypropyltriazolylmethyl) amine (THPTA), a water-soluble cuprous chelator which can ligate Cu(I) to protect it from oxidation. The effect of THPTA on the response of strains to CuNPs was similar to that of CAT, that is, the

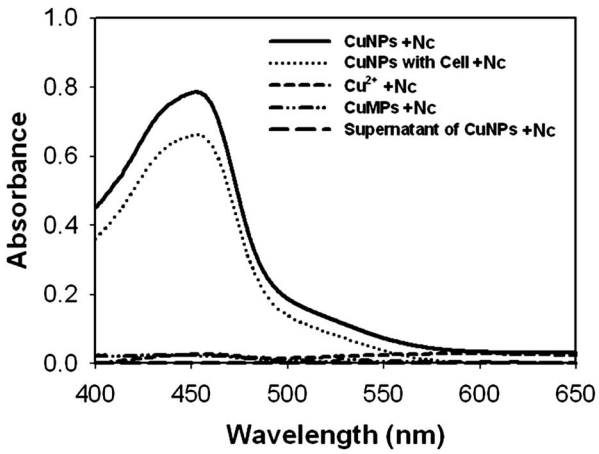

Fig. 6 Spectrophotometric determination of Cu(I) using Nc. The UV–vis absorption spectra are that of LB medium containing Nc and CuNPs with *E. coli* cells or without cells, or LB medium containing Nc and Cu(II), Nc and CuMPs, or Nc and the supernatant of CuNPs-containing medium.

responses of DPD2511 and other strains reduced 87% and 50–72%, respectively (Fig. 5), and the growth rate of RFM443 was by and large resumed when THPTA was added with CuNPs (Fig. S6†), whereas exposure to THPTA alone as a negative control did not affect luminescence signals of strains (Fig. S9†). Despite both Griffitt *et al.* and Midander *et al.* suggested that dissolution or the released particle fraction of copper nanoparticles accounted for only a small extent of CuNPs toxicity,[4,18] our above results show that the release of Cu(I) was responsible for the toxicity of CuNPs. Furthermore, the results that the stabilization of Cu(I) by THPTA almost abolished the response of DPD2511 and protected RFM443 suggest that there is a close relation between the oxidation of Cu(I) and the generation of H_2O_2, and the oxidation of the released Cu(I) may be the dominant route for H_2O_2 generation from CuNPs. The remaining response of strains after treatment with THPTA is probably due to H_2O_2 generation by the oxidation of components within the electron transport chain as a by-product of aerobic respiration,[34] which is not Cu(I)-dependent and thereby cannot be eliminated by THPTA. Hence, THPTA in the system protected Cu(I) from oxidation and inhibited a major part of H_2O_2 production, which resulted in the reduction of oxidative stress in the cells, the protection of biomacromolecules, and thus the reduction of responses of DPD2511, DPD2540, DPD2794, TV1061, and RFM443 to CuNPs. Comparatively, there was no obvious Cu(I) generated from CuMPs in similar analysis system (Fig. 6), which is in accordance with their non-toxicity. The results here confirm that H_2O_2 generation from CuNPs is Cu(I)-mediated and it causes multifaceted damages in cells and plays a significant role in toxicological effects of CuNPs.

3.5 Internalization of CuNPs

The small-size characteristics make nanoparticles easier to for the cells to internalize than bulk particles, and it was suggested that the high uptake of nanoparticles was a primary cause for the observed higher toxicity.[2,35,36] Here we wondered whether the internalization of CuNPs happened in the tested strains. A TEM of bacterial sample ultrathin sections allowed us to detect the morphology of the cells and the relative sites of CuNPs in the cells (Fig. 7). The morphology of cells grown with CuNPs in LB medium changed a lot, and many cells were shorter than normal rod-shaped ones in CuNPs-free LB medium (an average size of the normal rod-shaped *E. coli* is about 2 μm). It was highly probable that these cells lived under conditions that were bacteriostatic. Fig. 7 also shows that CuNPs are not only adsorbed on the cell surface but also internalized into the cells in 30 min, indicating rapid uptake of CuNPs by the cells. The dynamic light scattering (DLS) result showed that the hydrodynamic size of CuNPs suspended in LB medium is about 300 nm (Fig. S10†), which is about two times larger than the primary particle and suggests that CuNPs have a trend to agglomerate, the adsorbed and penetrated particles separated very well and retained their large specific surface area and ultrahigh surface activity to readily interact with the local biomolecules. Then the internalization of CuNPs will bring a Trojan horse toxicity effect and further aggravate cell damage, including damage of partial cell walls and cell membranes,

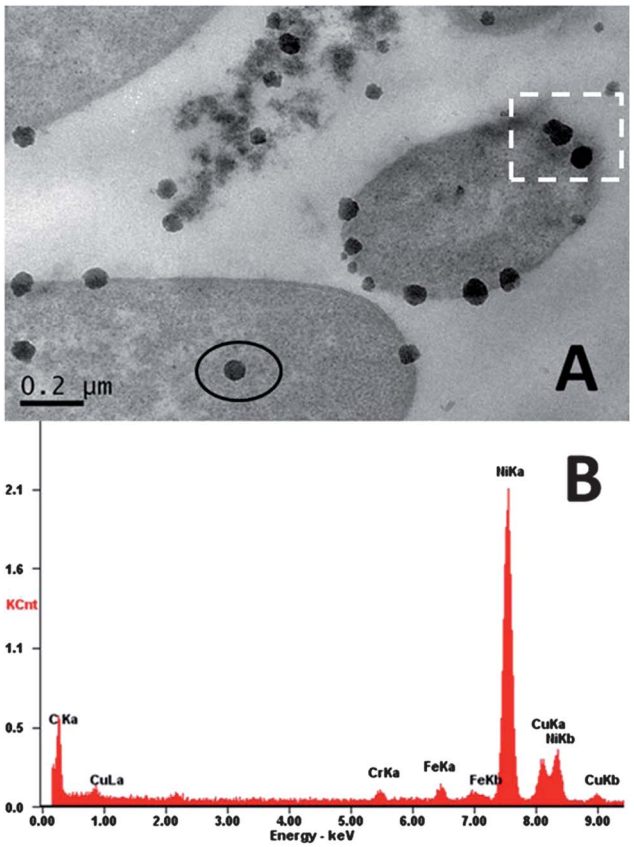

Fig. 7 (A) TEM image of *E. coli* cells after exposure to 80 mg L^{-1} CuNPs for 30 min. The dashed pane indicates the damage of cell wall and cell membrane. (B) EDX of the particle that is circled in Fig. 7A.

which were also found in Fig. 7 (the dashed pane). Because the membrane damage-sensitive strain, DPD2540, showed significant response to H_2O_2 generated from CuNPs (Fig. 4 and 5 and S6†), the cell membrane damage observed by TEM probably resulted from the CuNPs-induced ROS production.

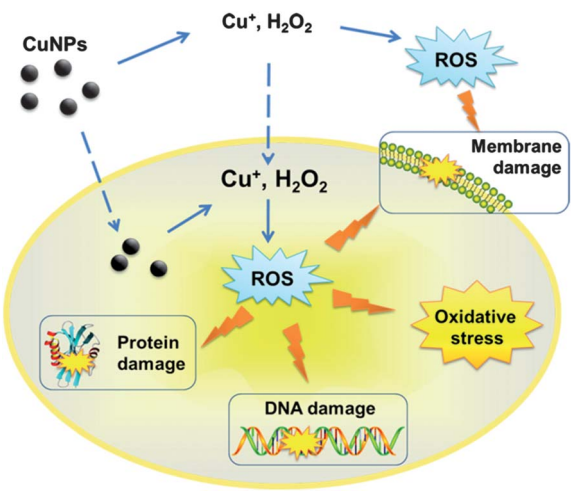

Scheme 1 A schematic representation of the primary toxic mechanism of CuNPs based on the results obtained.

The results above illustrated a preliminary but complicated mechanism of CuNPs toxicity both outside and inside the cell (Scheme 1). With a large specific surface area and high surface activity, CuNPs in the medium reveal a high initial release rate, and the soluble species, Cu(I) and Cu(II), coupled with such ROS as O^{2-} and H_2O_2, are produced. Then the continuously produced Cu(I) is rapidly oxidized, which leads to the generation of H_2O_2. Redox reactions between Cu(I) and Cu(II) will aggravate the toxicity of CuNPs, such as Cu(II) would be reduced to Cu(I) by O^{2-} (according to the Haber–Weiss Reaction[37]), and Cu(I) would trigger a Fenton-type reaction to transform H_2O_2 to the highly active hydroxyl radical (˙OH), which will readily and efficiently damage biomolecules. Besides the rapid release in the medium, these small-sized CuNPs are also adsorbed and incepted by the cell. Within the cell, CuNPs and their released copper ions interact with biomolecules to generate ROS,[38] which, together with the membrane permeable H_2O_2, lead to ROS accumulation and oxidative stress in *E. coli*, and modify various biomacromolecules, such as DNA and proteins. At the same time, ROS generated outside and inside the cell work together to damage the cell wall and membrane. The damage-caused leaks of the cell wall and membrane accelerate the internalization of CuNPs and further aggravate the cellular damage. Since CAT can diminish H_2O_2 and THPTA can stabilize Cu(I), both of them would protect cells against the multifaceted damages by CuNPs.

With a much smaller surface to volume ratio, CuMPs, compared to CuNPs, have relatively fewer atoms on their surfaces, and show less activity and much lower toxicity. The released copper from CuMPs was just about 1.3 mg L^{-1} in the first 30 min in LB (Fig. S8†), and cannot induce a significant toxic effect in *E. coli*. That there was little detectable Cu(I) produced from CuMPs (Fig. 6) can also partly explain the non-toxicity of CuMPs. Besides, CuMPs have similar size (or bigger size) to bacteria, making their internalization impossible. Thus the particle size is decisive to several properties of copper particles, including surface reactivity, internalization capacity, and toxicity.

Since dissolved Cu(II) leaching from CuO nanoparticles was identified as the source of toxicity to *E. coli* in a previous report,[32] the effect of soluble Cu(II) on the cell was compared to that of CuNPs in this study. We demonstrated that CuNPs induced more cytotoxicity than Cu(II) ions in all test concentrations (0–200 mg L^{-1}) (Fig. 3). Cu(II) caused detectable membrane damage, protein damage and slight DNA damage only at a high concentration (>140 mg L^{-1}). In comparison with Cu(II), CuNPs were able to induce much more intensive damages and a broader spectrum of toxic effects in test cells at low concentrations (maximum at 80 mg L^{-1}) (Fig. 4). One possible reason for the observed higher toxicity of CuNPs is that the CuNPs-caused H_2O_2 generation, the major source of CuNPs toxicity proven by our results, can happen both outside and inside of the cells, while Cu(II), like most heavy metals, has to enter the cell to produce physiological or toxic effects.[39] The other possible reason is that the metal nanoparticles were internalized by cells more efficiently than metal ions, and it has been reported that the CoNPs was taken up at a high rate by human leukocytes whereas the internalization of Co^{2+} was slow.[40] Moreover, the reduced damage of biomacromolecules from soluble Cu(II) in low concentration is probably due to the fact that *E. coli* has developed a multilevel copper ions defense mechanism to keep copper ions in homeostasis in the cell. These resistant systems include such copper ions transporters as ATPase CopA and CusCBFA system,[41,42] and the multicopper oxidase CueO.[43] ATPase CopA pumps cytoplasmic copper into the periplasm, and the proton-driven CusCBFA system further exports the periplasmic copper across the outer membrane.[41,42] CueO oxidizes Cu(I) to Cu(II) to protect the cell.[43] Therefore, only Cu(II) in high concentrations can overcome the resistance of this system, causing obvious cell damage. This resistance system specifically targets copper ions and probably cannot be efficient to excrete CuNPs.

The released copper fraction of CuNPs after immersion in LB for 30 min was also collected, named as supernatant of CuNPs, and analyzed for its effect on the bacteria. Although the amount of total released copper ions in the supernatant of CuNPs was detected by AAS, little Cu(I) can be detected by Nc in the collected supernatant (Fig. 6), possibly because Cu(I) is unstable in water systems and can easily be oxidized to Cu(II) during preparation of the sample (about 15 min). The supernatant of CuNPs cannot induce any obvious stress in the cells (Fig. S9†). AAS and inductively coupled plasma-mass spectrometry (ICP-MS) were always employed to quantify the amount of released ions from metal nanoparticles,[4,29,44,45] whereas these methods cannot differentiate the ions among their different valence states. Our study demonstrated that CuNPs affect the cell metabolism and growth mainly due to Cu(I)-mediated H_2O_2 generation, so it is proposed that, besides the elementary analysis for total ions measurement, the valence state analysis of the released ions from metal nanoparticles, especially transition metal nanoparticles, is also important when toxicity investigation and the relative toxic mechanism analysis of the nanoparticles are performed.

4 Conclusions

The toxicity of copper nanoparticles (CuNPs) was analyzed by using a stress-respective bacterial biosensor array. The toxicological effects of CuNPs can be quickly detected in about 30 min after exposure. The primary mechanism of toxicity of CuNPs was illustrated. CuNPs can induce multifaceted damages in the bacterial cells, including oxidative stress, DNA damage, protein damage, and membrane damage, which result in significant cytotoxicity. The releasing Cu(I)-mediated H_2O_2 generation from CuNPs is identified as the major source of toxicity of CuNPs. Internalization and adsorption of CuNPs were observed, which may aggravate cell damages. Compared with the rapid release and great toxicological effects of CuNPs, CuMPs are relative stable and do not release obvious Cu(I), which is consistent with their practically non-toxic properties. In addition, CuNPs can induce more intensive toxic effects and broader spectrum of cellular damages in much lower concentrations than soluble Cu(II) do. In addition, we found through this study that the release action of metal nanoparticles cannot be simply

characterized by the ion amount detection, but the valence state analysis of the released ions should also be considered, as it is closely related to the particle toxicity. Furthermore, the current work demonstrates that using the stress-responsive bacterial biosensor array is an effective short cut to screen the nanoparticles toxicity, to elucidate the toxicological effects of the nanoparticles, and to lift the curtain on the primary mechanism of the toxicity of the nanoparticles.

Acknowledgements

Authors appreciate Dr Shimshon Belkin at the Hebrew University for kindly providing the recombinant *E. coli* strains and Dr Haiyan Ren for help with writing. Financial support from the NSFC (No. 20907013 and 21190044), the 973 Program (2009CB421601), and the NSFHP (10JJ2005) is greatly acknowledged. This work is partly funded by the NSFC (No. 20805013, 20905024, 20975032, and 21075031), the open fund of SKLCBSC (KF2009-21) and PCSIRT.

Notes and references

1 J. M. Hillegass, A. Shukla, S. A. Lathrop, M. B. MacPherson, N. K. Fukagawa and B. T. Mossman, *Wiley Interdiscip. Rev.: Nanomed. Nanobiotechnol.*, 2010, **2**, 219–231.
2 S. J. H. Soenen and M. De Cuyper, *Contrast Media Mol. Imaging*, 2009, **4**, 207–219.
3 Z. Chen, H. Meng, G. Xing, C. Chen, Y. Zhao, G. Jia, T. Wang, H. Yuan, C. Ye, F. Zhao, Z. Chai, C. Zhu, X. Fang, B. Ma and L. Wan, *Toxicol. Lett.*, 2006, **163**, 109–120.
4 R. J. Griffitt, R. Weil, K. A. Hyndman, N. D. Denslow, K. Powers, D. Taylor and D. S. Barber, *Environ. Sci. Technol.*, 2007, **41**, 8178–8186.
5 N. A. Monteiro-Riviere, A. O. Inman and L. W. Zhang, *Toxicol. Appl. Pharmacol.*, 2009, **234**, 222–235.
6 R. Lei, C. Wu, B. Yang, H. Ma, C. Shi, Q. Wang, Q. Wang, Y. Yuan and M. Liao, *Toxicol. Appl. Pharmacol.*, 2008, **232**, 292–301.
7 A. Vollmer, S. Belkin, D. Smulski, T. Van Dyk and R. LaRossa, *Appl. Environ. Microbiol.*, 1997, **63**, 2566–2571.
8 S. Belkin, D. Smulski, A. Vollmer, T. Van Dyk and R. LaRossa, *Appl. Environ. Microbiol.*, 1996, **62**, 2252–2256.
9 O. Bechor, D. R. Smulski, T. K. Van Dyk, R. A. LaRossa and S. Belkin, *J. Biotechnol.*, 2002, **94**, 125–132.
10 T. K. Van Dyk, W. R. Majarian, K. B. Konstantinov, R. M. Young, P. S. Dhurjati and R. A. LaRossa, *Appl. Environ. Microbiol.*, 1994, **60**, 1414–1420.
11 N. Hever and S. Belkin, *Eng. Life Sci.*, 2006, **6**, 319–323.
12 S. Rodriguez-Mozaz, M. Lopez de Alda and D. Barceló, *Anal. Bioanal. Chem.*, 2006, **386**, 1025–1041.
13 M. B. Gu, J. Min and E. J. Kim, *Chemosphere*, 2002, **46**, 289–294.
14 E. T. Hwang, J. H. Lee, Y. J. Chae, Y. S. Kim, B. C. Kim, B.-I. Sang and M. B. Gu, *Small*, 2008, **4**, 746–750.
15 S. Magdassi, M. Grouchko and A. Kamyshny, *Materials*, 2010, **3**, 4626–4638.
16 G. Liu, X. Li, B. Qin, D. Xing, Y. Guo and R. Fan, *Tribol. Lett.*, 2004, **17**, 961–966.
17 N. Cioffi, N. Ditaranto, L. Torsi, R. A. Picca, L. Sabbatini, A. Valentini, L. Novello, G. Tantillo, T. Bleve-Zacheo and P. G. Zambonin, *Anal. Bioanal. Chem.*, 2005, **381**, 607–616.
18 K. Midander, P. Cronholm, H. L. Karlsson, K. Elihn, L. Möller, C. Leygraf and I. O. Wallinder, *Small*, 2009, **5**, 389–399.
19 B. M. Prabhu, S. F. Ali, R. C. Murdock, S. M. Hussain and M. Srivatsan, *Nanotoxicology*, 2010, **4**, 150–160.
20 J. M. Pettibone, A. Adamcakova-Dodd, P. S. Thorne, P. T. O'Shaughnessy, J. A. Weydert and V. H. Grassian, *Nanotoxicology*, 2008, **2**, 189–204.
21 J. C. Lewis, A. Feltus, C. M. Ensor, S. Ramanathan and S. Daunert, *Anal. Chem.*, 1998, **70**, 579A–585A.
22 S. Belkin, D. R. Smulski, S. Dadon, A. C. Vollmer, T. K. Van Dyk and R. A. Larossa, *Water Res.*, 1997, **31**, 3009–3016.
23 T. Xia, M. Kovochich, J. Brant, M. Hotze, J. Sempf, T. Oberley, C. Sioutas, J. I. Yeh, M. R. Wiesner and A. E. Nel, *Nano Lett.*, 2006, **6**, 1794–1807.
24 A. Nel, T. Xia, L. Mädler and N. Li, *Science*, 2006, **311**, 622–627.
25 T. Xia, M. Kovochich and A. Nel, *Clin. Occup. Environ. Med.*, 2006, **5**, 817–836.
26 H. Meng, T. Xia, S. George and A. E. Nel, *ACS Nano*, 2009, **3**, 1620–1627.
27 L. Macomber, C. Rensing and J. A. Imlay, *J. Bacteriol.*, 2007, **189**, 1616–1626.
28 P. Wick, P. Manser, P. Spohn, R. N. Grass, L. K. Limbach, A. Bruinink and W. J. Stark, *Environ. Sci. Technol.*, 2006, **40**, 4374–4381.
29 T. Xia, M. Kovochich, M. Liong, L. Maädler, B. Gilbert, H. Shi, J. I. Yeh, J. I. Zink and A. E. Nel, *ACS Nano*, 2008, **2**, 2121–2134.
30 V. Aruoja, H.-C. Dubourguier, K. Kasemets and A. Kahru, *Sci. Total Environ.*, 2009, **407**, 1461–1468.
31 N. Cioffi, L. Torsi, N. Ditaranto, G. Tantillo, L. Ghibelli, L. Sabbatini, T. Bleve-Zacheo, M. D'Alessio, P. G. Zambonin and E. Traversa, *Chem. Mater.*, 2005, **17**, 5255–5262.
32 C. Gunawan, W. Y. Teoh, C. P. Marquis and R. Amal, *ACS Nano*, 2011, **5**, 7214–7225.
33 H. H. Al-Sa'doni, I. L. Megson, S. Bisland, A. R. Butler and F. W. Flitney, *Br. J. Pharmacol.*, 1997, **121**, 1047–1050.
34 J. T. Greenberg, P. Monach, J. H. Chou, P. D. Josephy and B. Demple, *Proc. Natl. Acad. Sci. U. S. A.*, 1990, **87**, 6181–6185.
35 H.-J. Yen, S.-H. Hsu and C.-L. Tsai, *Small*, 2009, **5**, 1553–1561.
36 H.-H. Chen, C.-C. Chien, C. Petibois, C.-L. Wang, Y. Chu, S.-F. Lai, T.-E. Hua, Y.-Y. Chen, X. Cai, I. Kempson, Y. Hwu and G. Margaritondo, *Nanobiotechnol*, 2011, **9**, 14.
37 M. Chevion, *Free Radical Biol. Med.*, 1988, **5**, 27–37.
38 A. V. Kachur, C. J. Koch and J. E. Biaglow, *Free Radical Res.*, 1998, **28**, 259–269.
39 D. H. Nies, *Appl. Microbiol. Biotechnol.*, 1999, **51**, 730–750.

40 R. Colognato, A. Bonelli, J. Ponti, M. Farina, E. Bergamaschi, E. Sabbioni and L. Migliore, *Mutagenesis*, 2008, **23**, 377–382.
41 C. Rensing, B. Fan, R. Sharma, B. Mitra and B. P. Rosen, *Proc. Natl. Acad. Sci. U. S. A.*, 2000, **97**, 652–656.
42 S. Franke, G. Grass, C. Rensing and D. H. Nies, *J. Bacteriol.*, 2003, **185**, 3804–3812.
43 S. K. Singh, G. Grass, C. Rensing and W. R. Montfort, *J. Bacteriol.*, 2004, **186**, 7815–7817.
44 P. Cronholm, K. Midander, H. L. Karlsson, K. Elihn, I. O. Wallinder and L. Möller, *Nanotoxicology*, 2011, **5**, 269–281.
45 B. Wu, Y. Wang, Y.-H. Lee, A. Horst, Z. Wang, D.-R. Chen, R. Sureshkumar and Y. J. Tang, *Environ. Sci. Technol.*, 2010, **44**, 1484–1489.
46 X.-M. Liu, A. Thakur and D. Wang, *Biomacromolecules*, 2007, **8**, 2653–2658.

